

# HD molecules in Milky Way

© D.N. Kosenko, S.A. Balashev

loffe Institute,  
194021 St. Petersburg, Russia  
e-mail: kosenkodn@yandex.ru

Received May 12, 2023

Revised July 31, 2023

Accepted October, 30, 2023

We have provided an independent analysis of HD and H<sub>2</sub> absorption lines in several systems in our Galaxy using FUSE space telescope archival data and neutral carbon and metal lines in these systems using HST archival data. The obtained HD column densities lie in the range from  $\sim 10^{14}$  to  $\sim 10^{16}$  cm<sup>-2</sup>. The obtained column densities were used to estimate physical conditions in the analyzed systems, including cosmic ray ionization rate, which were obtained in the range from  $\xi \sim 10^{-17}$  to  $\sim 10^{-15.5}$  s<sup>-1</sup>.

**Keywords:** galaxies, Interstellar medium, cosmic rays.

DOI: 10.61011/TP.2023.12.57735.f212-23

## Introduction

Molecular hydrogen, H<sub>2</sub>, — is the most abundant molecule in the Universe, being a tracer of the cold phase of the neutral interstellar medium (ISM). With a sufficiently large abundance of H<sub>2</sub> in the medium, it is also possible to detect its isotopomer, the molecule HD. Inasmuch as the intrinsic emission of the molecules H<sub>2</sub> and HD is suppressed, the main method of studying these molecules in the interstellar medium — is spectroscopy of absorption lines in the direction of bright background sources. However, atmospheric absorption prevents ground-based telescopes from observing H<sub>2</sub> and HD absorption lines in the Milky Way and neighboring galaxies, inasmuch as these absorption lines are in the ultraviolet region of the spectrum ( $\lambda \lesssim 1100$  Å). Therefore, data from space telescopes such as FUSE and Copernicus are used to observe these molecules in the local universe.

Previously, archival data from the FUSE Space Telescope were used to study H<sub>2</sub> and HD in our Galaxy and in the Magellanic Clouds [1–3], but the paper [1] presents only a fraction of the absorption systems of the Milky Way where molecules HD have been identified. In addition, for many of the systems where the molecule lines H<sub>2</sub> have been found, archival data from the Hubble Space Telescope (HST) are available, allowing the study of neutral carbon, CI lines, as well as the estimation of metallicity in the system. Using the column density<sup>1</sup> HD, as well as the populations of H<sub>2</sub> rotational levels, CI fine-structure levels, and the metallicities, it is possible to estimate the physical conditions in the system, namely the ultraviolet (UV) background intensity,  $\chi$ , the number density,  $n$ , and the cosmic ray ionization rate,  $\xi$ , which determine the chemical evolution of the cloud (see, e.g., [4]).

In the presented pilot work, we selected eight absorption systems towards the stars of our Galaxy, in five of which

HD lines have not yet been studied. For a homogeneous analysis, we re-analyzed the H<sub>2</sub> lines, and also found populations of CI fine-structure levels and metallicities in these systems, as described in Sec. 2, the results are discussed in Section 2. In Section 3, using the obtained column density, we performed estimates for the physical conditions mentioned above in the environment associated with absorption systems.

## 1. Data & Analysis

In this work, archival data from the FUSE [5,6] space telescope were used. We selected a subsample of systems from the sample provided by [2] to analyze possible systematic effects in previous HD measurements, as well as to search for new systems containing HD.

The FUSE spectra are poorly calibrated in terms of wavelength, so we applied a procedure to improve the quality of the calibration [7]. To do this, we compared the lines H<sub>2</sub> in the observed spectrum with the corresponding lines in the synthetic spectrum (only thin, single lines were taken) and the shift between them was estimated by cross-correlation [8]. The shift was further built as a function of the wavelength, which was used to adjust the calibration of the exposures when they were added. Also, the addition of individual exposures made it possible to significantly improve the ratio of signal to noise ratio of the spectrum, which was  $S/N \sim 20$ –50 in the considered systems.

To fit the absorption lines, we used a multicomponent Voigt profile (components are defined by the velocity shift), which gives estimates of column density,  $N$ , and Doppler parameters,  $b$ , for different levels. We observed that as a result of the procedure of calibration and addition of exposures, as well as other systematic effects, the spectral resolution can deteriorate (nominal resolution FUSE  $R = \lambda/\Delta\lambda = 20\,000$ ), so it was a free parameter when fitting. To determine the posterior distributions of the parameters, Bayesian analysis with Markov Chain the Monte-Carlo sampling was used.

<sup>1</sup> Hereinafter, the column density (denoted  $N$ ) is measured in cm<sup>-2</sup>.

**Table 1.** HD, H<sub>2</sub> and CI column density measurements

Star	$v_{\text{LSR}}^a$ , km/s	$\log N_{\text{HI}}^b$	$\log N_{\text{H}_2}$	$\log N_{\text{HD}}$	$\log N_{\text{CI}}$
HD 93129A	−39.1	21.47	$16.70^{+0.08}_{-0.35}$	$\lesssim 13.4$	$13.93^{+0.02}_{-0.01}$
	−16.8	„–“	$18.22^{+0.11}_{-0.08}$	$\lesssim 13.9$	$14.61^{+0.01}_{-0.01}$
	1.0	„–“	$20.22^{+0.01}_{-0.01}$	$16.33^{+0.11}_{-0.32}$	$14.80^{+0.01}_{-0.01}$
HD 93205	−83.8	21.36	$16.67^{+0.07}_{-0.12}$	$\lesssim 13.1$	$13.68^{+0.01}_{-0.01}$
	3.6	„–“	$19.80^{+0.01}_{-0.01}$	$15.74^{+0.19}_{-0.14}$	$14.80^{+0.01}_{-0.01}$
HD 93843	$\sim 2.5$	21.3	$19.68^{+0.01}_{-0.01}$	$14.12^{+0.08}_{-0.04}$	$14.30^{+0.01}_{-0.01}$
HD 99890	−13.4	21.12	$19.56^{+0.01}_{-0.02}$	$14.28^{+0.01}_{-0.01}$	$14.58^{+0.01}_{-0.01}$
HD 100199	$\sim 2.8$	21.18	$20.21^{+0.01}_{-0.01}$	$14.49^{+0.22}_{-0.13}$	$14.70^{+0.01}_{-0.01}$
HD 101190	$\sim 3.9$	21.15	$20.47^{+0.02}_{-0.02}$	$16.45^{+0.07}_{-0.05}$	$15.11^{+0.03}_{-0.04}$
HD 103779	$\sim -2.9$	21.17	$19.95^{+0.06}_{-0.01}$	$14.10^{+0.04}_{-0.03}$	$14.48^{+0.01}_{-0.01}$
HD 104705	−21.8	21.15	$18.43^{+0.03}_{-0.04}$	$13.87^{+0.34}_{-0.20}$	$13.82^{+0.01}_{-0.01}$
	2.9	„–“	$20.02^{+0.01}_{-0.01}$	$15.2^{+0.32}_{-0.33}$	$14.39^{+0.01}_{-0.01}$

Note. <sup>a</sup> — absorption systems velocity relative to the local standard of rest, <sup>b</sup> — values are taken from [2].

In addition, we used two penalty functions to adjust the smoothness of the shape of H<sub>2</sub> rotational level number, and to increase the Doppler parameter with increasing rotational level number H<sub>2</sub> (for observations of this effect, see, e.g., [9]). For a detailed description of the method used, see in papers [4,10].

At the velocities corresponding to the positions of the H<sub>2</sub> components in the spectrum, we searched for molecules HD. In the case where we could only set the upper limit (herein further the upper and lower limits are determined from the analysis of the aposterior distribution function at the level of  $3\sigma$ ) on the HD column density, the positions of the lines were fixed and the priors on the Doppler parameters obtained in the analysis of the lines H<sub>2</sub> were used.

Using archival HST data, we also analysed the CI and metal absorption lines, which was necessary for the assessment of physical conditions. In the analysis of the CI lines, it was assumed that all levels of the fine structure have an identical Doppler parameter.

## 2. Results

Estimates of column density of HD, H<sub>2</sub>, and CI are presented in Table 1. Systems towards HD 93205, HD 101190, and HD 104705 have been previously studied [1]. The found value of  $\log N_{\text{HD}}$  in the direction of HD 104705 is close to what yields [2], but for HD 93205 and HD 101190 the values differ by order. Such a difference may be the result of different approaches to data processing: [1] used the method of constructing a curve of growth to determine  $b$  and  $N$ , while we used the method of fitting with a multicomponent Voigt profile. In addition, for HD 93205

in [1], the lower limit on  $b$  was obtained on the assumption that the line is optically thin and in the linear region of the curve of growth, which excludes saturated solutions. Thus, we have detected HD molecules in five new systems in our Galaxy. Fig. 1 shows a comparison of the obtained column density of HD and H<sub>2</sub> with known measurements at high redshifts [4], in the Magellanic Clouds [16] and isotopic ratio D/H. Also shown for comparison are the values obtained earlier for our Galaxy [1]. The large variation in the obtained values can be explained by the different physical conditions in the observed systems and the high sensitivity of the concentration HD to their change [11]. We previously showed that the ratio  $N_{\text{HD}}/N_{\text{H}_2}$  decreases as metallicity increases, as the concentration of ionized hydrogen, which is necessary for the formation of HD in the gas phase, decreases. Nevertheless,  $N_{\text{HD}}/2N_{\text{H}_2} > \text{D}/\text{H}$  ratios were detected in three systems, which may indicate, for example, an increased flux of cosmic rays.

## 3. Physical conditions

Using estimates for column density H<sub>2</sub>, HD, and CI, we performed estimates of the physical conditions in the environment associated with absorption systems according to the procedure proposed and used earlier for HD/H<sub>2</sub> systems at cosmological redshifts in the work [4].

According to this procedure,  $n$  and  $\chi$  are estimated from the joint analysis of H<sub>2</sub> rotational and CI fine-structure level populations based on a comparison of the observed values with the model grids calculated by the code MEUDON PDR [12,13]. Then we constrain  $\xi$  using the semi-analytical model described in [11]. It was shown that the ratio of column density HD and H<sub>2</sub> depends on  $\xi$ ,

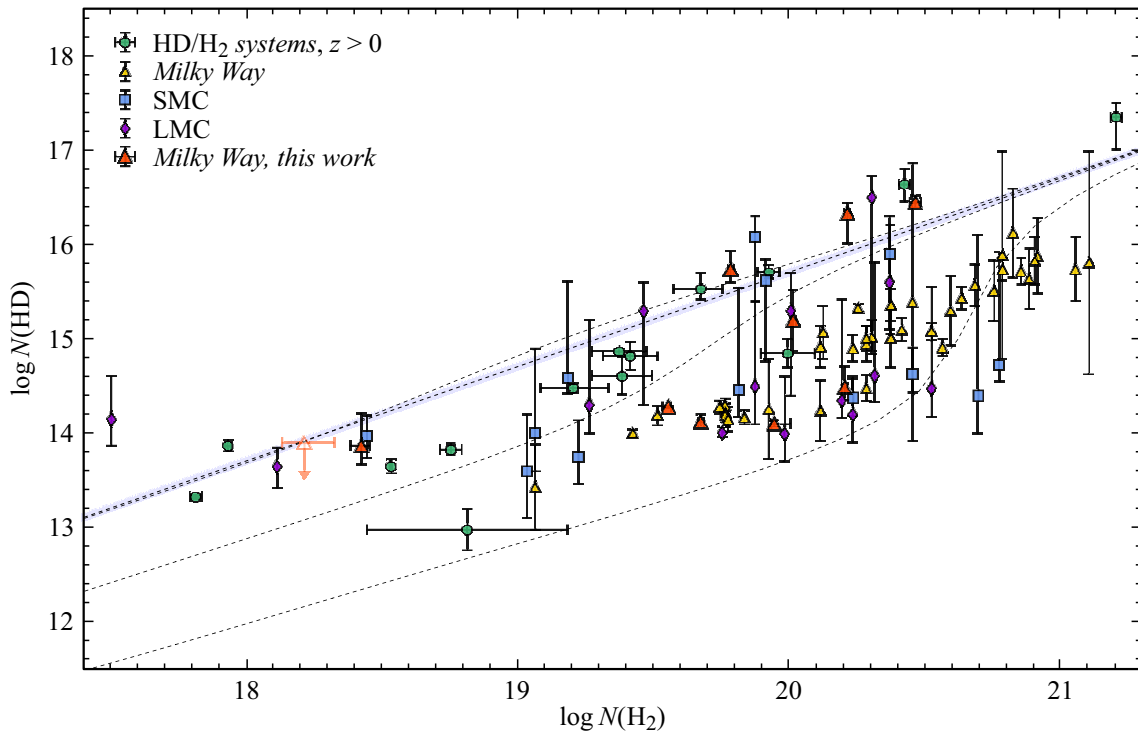


**Figure 1.** Measured HD and H<sub>2</sub> column densities. The results obtained in this work are indicated by red triangles, yellow triangles show HD measurements in our Galaxy obtained earlier in [1], green circles indicate measurements at high redshifts [4], blue squares — in Small Magellanic Cloud, purple diamonds — in Large Magellanic Cloud. The light blue line shows the value of the primary isotopic ratio D/H [15]. Dotted curves — theoretical calculations of the HD/H<sub>2</sub> ratio for log  $\xi = -15, -16, -17$ .

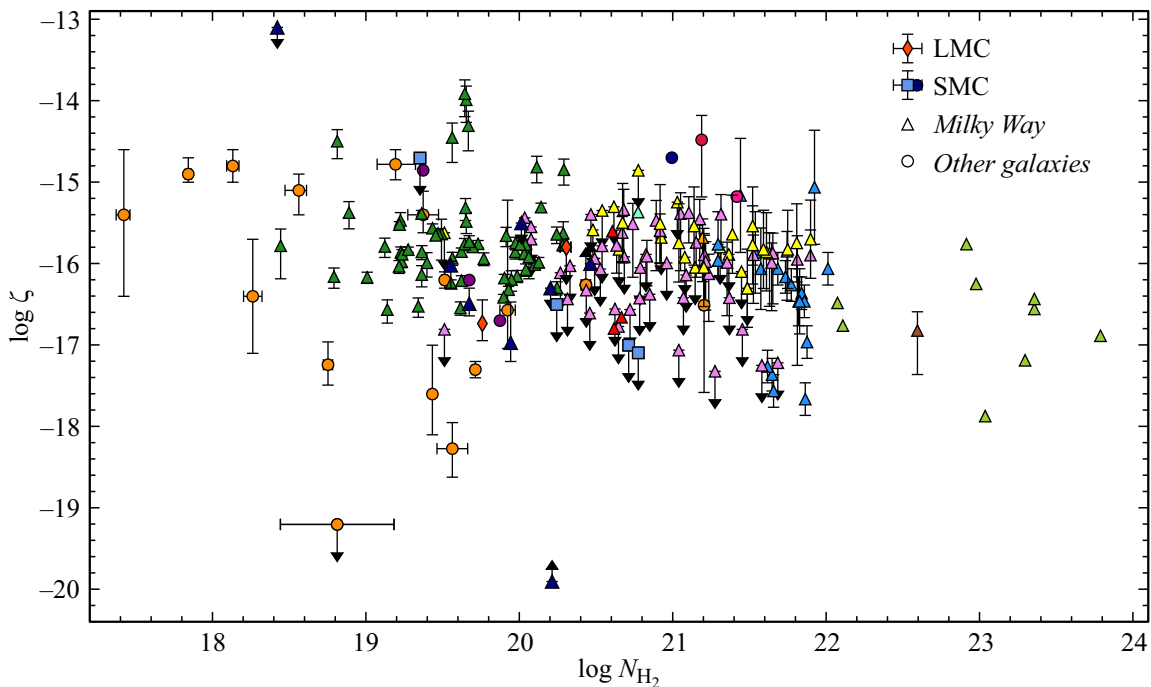


**Figure 2.** Cosmic Ray Ionization Rate as a Function of Column Density H<sub>2</sub>. Triangles — are estimates obtained in our Galaxy (dark blue dots were obtained in this paper), squares — in Small Magellanic Cloud, diamonds — in Large Magellanic Cloud, circles — in other galaxies (references, e.g., in [4]).

**Table 2.** Constraints of physical conditions

Star	$v_{\text{LSR}}$ , km/s	$[X/H]$	X	$\log n$ , $\text{cm}^{-2}$	$\log \chi$	$\log \xi$ , $\text{s}^{-1}$
HD 93129A	−39.1	$-0.28^{+0.05}_{-0.05}$	Zn	$2.98^{+0.31}_{-0.35}$	$0.69^{+0.26}_{-0.24}$	—
	−16.8	„—“	„—“	$2.65^{+0.35}_{-0.22}$	$1.58^{+0.48}_{-0.23}$	—
	1.0	„—“	„—“	$1.63^{+0.17}_{-0.19}$	$0.48^{+0.29}_{-0.21}$	$\gtrsim 19.9$
HD 93205	−83.8	$0.11^{+0.06}_{-0.06}$	S	$\gtrsim 2.5$	$1.51^{+0.68}_{-0.33}$	—
	3.6	„—“	„—“	$1.32^{+0.17}_{-0.17}$	$0.44^{+0.36}_{-0.26}$	—
HD 93843	$\sim 2.5$	$-0.03^{+0.04}_{-0.04}$	P	$1.77^{+0.16}_{-0.16}$	$0.52^{+0.19}_{-0.18}$	$-16.49^{+0.19}_{-0.15}$
HD 99890	−13.4	$0.07^{+0.03}_{-0.03}$	P	$1.42^{+0.17}_{-0.16}$	$1.29^{+0.44}_{-0.40}$	$-16.02^{+0.65}_{-0.28}$
HD 100199	$\sim 2.8$	$0.01^{+0.10}_{-0.04}$	P	$1.70^{+0.18}_{-0.18}$	$0.44^{+0.23}_{-0.20}$	$\lesssim -16.3$
HD 101190	$\sim 3.9$	$-0.11^{+0.05}_{-0.05}$	Zn	$1.76^{+0.18}_{-0.17}$	$0.59^{+0.23}_{-0.18}$	$\gtrsim -16.0$
HD 103779	$\sim 2.9$	$-0.02^{+0.08}_{-0.06}$	S	$1.27^{+0.17}_{-0.17}$	$0.59^{+0.44}_{-0.24}$	$-16.97^{+0.50}_{-0.23}$
HD 104705	−21.8	$0.10^{+0.03}_{-0.03}$	P	$1.05^{+0.14}_{-0.15}$	$1.04^{+0.47}_{-0.31}$	$\lesssim -13.1$
	2.9	„—“	„—“	$1.28^{+0.18}_{-0.19}$	$0.23^{+0.31}_{-0.22}$	$\lesssim -15.5$

Note. Columns: (i) the name of the star; (ii) the velocity of the absorption system relative to the local standard of rest; (iii) metallicity; (iv) an element for assessing metallicity; (v) number density; (vi) the intensity of UV radiation; (vii) the rate of ionization by cosmic rays. In the direction of HD 93129A (1 and 2 components) and HD 93205, the cosmic ray ionization rate was not estimated.

$n$ ,  $\chi$  and metallicity  $Z$  (which was determined from the analysis of metal lines in the HST spectra and fixed in further calculations). We used Markov Chain Monte-Carlo method to determine  $\xi$ , and the values  $n$  and  $\chi$  found from  $\text{H}_2$  and CI were used as priors. The results are shown in the Table 2.

The obtained values of the cosmic ray ionization rate lie in a wide range  $\xi \sim 10^{-17} - 10^{-15.5} \text{ s}^{-1}$ , but are in good agreement with typical values in the diffuse phase of the ISM (see, e.g., review [14]).

## Funding

This paper was supported by grant of the Russian Science Foundation № 22-22-00164.

## Conflict of interest

The authors declare that they have no conflict of interest.

## References

- [1] T.P. Snow, T.L. Ross, J.D. Destree, M.M. Drosback, A.G. Jensen *ApJ*, **688**, 1124 (2008). DOI: 10.1086/592288
- [2] J.M. Shull, C.W. Danforth, K.L. Anderson. *ApJ*, **911**, 55 (2021). DOI: 10.3847/1538-4357/abe707
- [3] D.E. Welty, R. Xue, T. Wong. *Astrophys. J.*, **745**, 173 (2012). DOI: 10.1088/0004-637X/745/2/173
- [4] D.N. Kosenko, S.A. Balashev, P. Noterdaeme, J.-K. Krogager, R. Srianand, C. Ledoux. *MNRAS*, **505**, 3810 (2021). DOI: 10.1093/mnras/stab1535
- [5] H.W. Moos, W.C. Cash, L.L. Cowie, A.F. Davidsen, A.K. Dupree, et al. *ApJ*, **538**, L1 (2000). DOI: 10.1086/312794
- [6] D.J. Sahnou, H.W. Moos, T.B. Ake, J. Andersen, B.G. Andersson, et al. *ApJ*, **538**, L7 (2000). DOI: 10.1086/312794
- [7] D.N. Kosenko, S.A. Balashev. *MNRAS* **525**, 2820 (2023). DOI: 10.1093/mnras/stad2299
- [8] S.M. Simkin. *A&A*, **31**, 129 (1974).
- [9] S.A. Balashev, D.A. Varshalovich, A.V. Ivanchik. *Astronomy Lett.*, **35**, 150 (2009). DOI: 10.1134/S1063773709030025
- [10] P. Noterdaeme, S.A. Balashev, J.-K. Krogager, R. Srianand, H. Fathivavsari, et al. *A&A*, **627**, A32 (2019). DOI: 10.1051/0004-6361/201935371
- [11] S.A. Balashev, D.N. Kosenko. *MNRAS: Lett.*, **492**, L45 (2020). DOI: 10.1093/mnrasl/slz180
- [12] F. Le Petit, C. Nehmé, J. Le Bourlot, E. Roueff. *Astrophys. J. Supplement Series*, **164**, 506 (2006). DOI: 10.1086/503252
- [13] V.V. Klimenko, S.A. Balashev. *MNRAS*, **498**, 1531 (2020). DOI: 10.1093/mnras/staa2134
- [14] M. Padovani, A.V. Ivlev, D. Galli, S.S.R. Offner, N. Indriolo, D. Rodgers-Lee, A. Marcowith, P. Girichidis, A.M. Bykov, J.M.D. Kruijssen. *Space Sci. Rev.*, **216**, 29 (2020). DOI: 10.1007/s11214-020-00654-1
- [15] Planck Collaboration, N. Aghanim, Y. Akrami, M. Ashdown, J. Aumont, C. Baccigalupi, et al. *A&A*, **641**, A6 (2020). DOI: 10.1051/0004-6361/201833910
- [16] D.N. Kosenko, S.A. Balashev *Cold diffuse interstellar medium of Magellanic Clouds: I. HD molecule and cosmic ray ionization rate*, *MNRAS*, 2023, vol.525, p.2820–2833, DOI: 10.1093/mnras/stad2299

Translated by 123